

## Research Article

# Blur2Sharp: A GAN-Based Model for Document Image Deblurring

Hala Neji<sup>1,2,3,\*</sup>, Mohamed Ben Halima<sup>2</sup>, Tarek. M. Hamdani<sup>2</sup>, Javier Noguera-Iso<sup>3</sup>, Adel M. Alimi<sup>2,4</sup>

<sup>1</sup>National Engineering School of Gabes (ENIG), University of Gabes, Gabes, Tunisia

<sup>2</sup>REGIM Lab (Research Groups in Intelligent Machines), University of Sfax, National Engineering School of Sfax (ENIS), Sfax, Tunisia

<sup>3</sup>Aragon Institute of Engineering Research (I3A), University of Zaragoza, Zaragoza, Spain

<sup>4</sup>Department of Electrical and Electronic Engineering Science, Faculty of Engineering and the Built Environment, University of Johannesburg, Johannesburg, South Africa

## ARTICLE INFO

### Article History

Received 16 Jan 2021

Accepted 25 Mar 2021

### Keywords

Generative adversarial network (GAN)  
Cycle-consistent generative adversarial network (CycleGAN)  
Document deblurring  
Blind deconvolution  
Motion blur  
Out-of-focus blur

## ABSTRACT

The advances in mobile technology and portable cameras have facilitated enormously the acquisition of text images. However, the blur caused by camera shake or out-of-focus problems may affect the quality of acquired images and their use as input for optical character recognition (OCR) or other types of document processing. This work proposes an end-to-end model for document deblurring using cycle-consistent adversarial networks. The main novelty of this work is to achieve blind document deblurring, i.e., deblurring without knowledge of the blur kernel. Our method, named “Blur2Sharp CycleGAN,” generates a sharp image from a blurry one and shows how cycle-consistent generative adversarial networks (CycleGAN) can be used in document deblurring. Using only a blurred image as input, we try to generate the sharp image. Thus, no information about the blur kernel is required. In the evaluation part, we use peak signal to noise ratio (PSNR) and structural similarity index (SSIM) to compare the deblurring images. The experiments demonstrate a clear improvement in visual quality with respect to the state-of-the-art using a dataset of text images.

© 2021 The Authors. Published by Atlantis Press B.V.

This is an open access article distributed under the CC BY-NC 4.0 license (<http://creativecommons.org/licenses/by-nc/4.0/>).

## 1. INTRODUCTION

Thanks to mobile technology we are able to capture documents in a simple way and at any moment. Text documents such as bank documents, advertisements, courier receipts, hand-written notes, digitized receipts, public information signboards, and information panels captured by portable cameras are very common in our daily lives. Portable cameras offer great conveniences for acquiring and memorizing information as they provide a new alternative for document acquisition in less constrained imaging environments than personal scanners. However, due to the variations in the imaging conditions as well as the target document type, there are many factors that can degrade the images such as image blurring, sharing distortions, geometrical warping, or noise pollution. Frequently, the motion blur caused by camera shake and the out-of-focus blur can affect the quality of the images obtained by mobile devices. Although blur may be not very relevant at first sight, it may be the cause of problems in ulterior processing tasks such as text segmentation or optical character recognition (OCR). Thus, traditional scanner-based OCR systems cannot be directly applied on camera-captured images and a new level of processing needs to be addressed.

The objective of this work is to study a new model for removing different types of blur from real blurry document images and generate the correspondent sharp images. Figure 1 illustrates the difference between source blur images (right) and sharp images (left).

Various deblurring techniques have been proposed so far based on blur kernel estimation: blind deconvolution methods and nonblind deconvolution methods. In nonblind deconvolution methods, we have some knowledge about the blur kernel. In contrast, in blind deconvolution methods no information about the blur kernel is known. Blind deblurring estimates a latent sharp image and a kernel blur, namely point spread function (PSF), from a blurred image. This problem has been deeply studied (see Section 2). However,

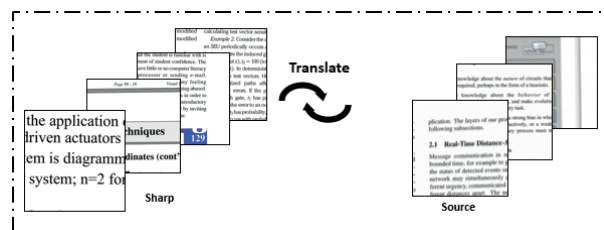


**Figure 1** | Examples of real source images with blur (right) and sharp images (left).

\* Corresponding author. Email: [hala.neji@ieee.org](mailto:hala.neji@ieee.org)

generic methods have not been effective with real world blurred images.

The proposal of this work is to eliminate blur and restore blurred images that are captured by low-cost camera devices without the best conditions. For this purpose, we propose to extend a cycle-consistent generative adversarial network (CycleGAN) for translating a blurred input text image into a sharp one. Recent methods based on generative adversarial networks (GAN) for tasks such as image-to-image translation [1] depend on the availability of training examples where the same data is available in both domains. However, CycleGAN [2] is able to learn such pair information without one-to-one mapping between training data in source and target domains. The challenge of this work is to propose a new architecture based on CycleGAN, which we call “Blur2Sharp CycleGAN,” for the task of text document deblurring. Blur2Sharp CycleGAN adjusts the parameters of CycleGAN that best fit the purpose of document deblurring.

The rest of this work is organized as follows. Section 2 reviews the state-of-the-art in blind deconvolution methods. Section 3 describes our suggested system. The evaluation and experimental results are provided in section 4. Finally, section 5 provides some concluding remarks.

## 2. STATE-OF-THE-ART

Given its wide range of applications, document image deblurring has attracted considerable attention in recent years, and various approaches have been proposed, overall in the field of blind deconvolution methods.

In blind deconvolution methods, the first task is to estimate the blur kernel. After this, the second part of the method is to restore the final latent image thanks to a nonblind deblurring algorithm. With the assumption that the blur is uniform and spatially invariant, the mathematical formulation of the blurry image can be modeled as  $Y = X * K + \epsilon$ , where  $X$  is a latent sharp image,  $K$  is an unknown blur kernel,  $*$  denotes the convolution operator,  $\epsilon$  is the additive noise and  $Y$  is the blurred observation.

Chen *et al.* [3] suggested an effective document image deblurring algorithm based on a Bayesian method that analyzes the local structure of a document image and uses an intensity probability density function as prior for deblurring. However, it is not generally applicable to blurred text images because it depends on text segmentation. Cho *et al.* [4] proposed another Bayesian method that takes into account more specific properties of text documents. Pan *et al.* [5] proposed another approach for text de-blurring that makes profit of L0 regularized intensity and gradient priors. Nayef *et al.* [6] suggested a method for document image deblurring that uses sparse representations improved by nonlocal means. Zhang *et al.* [7] used a gradient histogram preservation strategy for document image deblurring.

More recently, Ljubenovic *et al.* [8] proposed the use of a dictionary-based prior for class-adapted blind deblurring of document images. Using a large set of motion blurred images with the associated ground-truth blur kernels, Pan *et al.* [9] proposed a method to learn data fitting functions. Last, Jiang *et al.* [10]

proposed a method based on the two-tone prior for text image deblurring.

Convolutional neural networks (CNNs) have been also applied to various image enhancement tasks [11,12]. Focusing on text image deblurring, Hradiš *et al.* [13] proposed an end-to-end method to generate sharp images from blurred ones using CNN. Their network, consisting of 15 convolutional layers, is trained on 3 classes (blur, sharp image and kernel blur), but there are some disadvantages: on the one hand, pairwise images are required to train the networks; on the other hand, the result of deblurring is not appropriate for natural images which have a color background. Pan *et al.* [14] presented a genetic approach with two main ideas: modify the prior to assume that the dark channel of natural images is sparse instead of zero, and impose the sparsity for kernel estimation. They used CNN to predict the blur kernel.

In the past few years, generative adversarial networks (GANs) have been used in different image-related applications [15] such as generating synthetic data, style transfer, super-resolution, denoising, deblurring or text-to-image generation. For instance, Lee *et al.* [16] used GAN for progressive semantic face deblurring to reduce the motion blur on input face images. Guo *et al.* [17] proposed a GAN-based method for video deblurring with the objective to improve visual object tracking. More related to document deblurring, Xu *et al.* [18] proposed a method for jointly deblurring and super-resolving face and text images that are typically degraded by out-of-focus blur. Nimisha *et al.* [19] also used GAN for end-to-end deblurring network: using adversarial loss, the network learns a strong prior on the clean image domain and it maps the blurred image to its clean equivalent one. Inspired also on GAN architectures, Lu *et al.* [20] presented an unsupervised method for domain-specific single-image deblurring that tries to disentangle the content features and the blur features in blurred images.

In summary, the previous approaches cannot be generalized to deal with different scenarios in text document deblurring. Therefore, it is a challenging task to count on a method based on deep learning for building a general image prior that is able to handle different scenarios.

## 3. PROPOSED METHOD

Image deblurring aims to restore a clean image from a blurred one. As mentioned in the introduction, this work explores the feasibility of applying CycleGAN [2] with a new architecture for the challenging task of cleaning blurred text images. We want to demonstrate that CycleGAN approach is suitable for the simpler task of text image deblurring where the results are good. Our idea is that if we can treat blur and sharpness as a kind of image style, successful image deblurring may be achieved with unpaired image dataset based on CycleGAN.

The main advantage of CycleGAN is that it does not require a pairwise image dataset. To solve the issue of not having a ground-truth document of every input, CycleGAN proposes a reverse mapping function  $G_y$ . If a generator function  $G_x$  translates a document from domain  $X$  to domain  $Y$  just changing the appearance, it should be possible to map the image back to domain  $X$  with another generator function  $G_y$  and reconstruct the initial image:  $X \rightarrow G_x(X) \rightarrow G_y(G_x(X)) \approx X$ . The functions could be also reversely applied,

$Y \rightarrow G_Y(Y) \rightarrow G_X(G_Y(Y)) \approx Y$ , and no ground-truth documents should be needed for deblurring. The model contains also the associated adversarial discriminators  $D_Y$  and  $D_X$ .  $D_Y$  encourages  $G_X$  to translate  $X$  into outputs indistinguishable from domain  $Y$ , and vice-versa for  $D_X$  and  $G_Y$ . To further regularize the mappings, we introduce two cycle consistency losses that capture the intuition that if we translate from one domain to the other and back again we should arrive at where we started. Figure 2 shows a schema of this model that allows us to train our network with unpaired images to translate from blur to sharp or inversely.

Figure 3 shows the training process of our proposed Blur2Sharp CycleGAN. It consists of two generators and two discriminators. The main goal of generators is to learn the mapping between two image domains. In addition, the two adversarial discriminators aim to distinguish between images and translated images in the same way as they aim to discriminate between the sharp images and the generated images. The following subsections explain the details of the generative and discriminator networks.

### 3.1. Generative Network

As shown in Figure 4, both generators consist of three parts: an encoder, a transformer and a decoder. This figure summarizes the architecture of these three parts, which has shown good performance for image deblurring.

**Encoder** The input of the network is  $[256, 256, 3]$ . There are 3 layers to extract the features from an image by one stride each time. In the first layer each filter is  $7 \times 7$  and the stride is  $1 \times 1$ . The activation function is *ReLU*. The shape of the output is  $[256, 256, 64]$  (by padding). Then, the output of the first layer is passed to the following layers. The hyper-parameters of the second layer are: 128 filters where each filter is  $3 \times 3$  with stride 2; the activation function is *ReLU*; and the output is  $[128, 128, 128]$ . The hyperparameters of the third layer are: 256 filters where each filter is  $3 \times 3$  with stride 2; the activation function is *ReLU*; and the output is  $[64, 64, 256]$ .

**Transformer** The transformer aims to transform feature vectors of an image from one domain to another domain. The input is  $[64, 64, 256]$ . We started building our model from scratch. We started with 9 layers of *ResNet* blocks. However, as we did not obtain good results, we tried to change the model structure to improve the result. After testing different possibilities, we chose the hyperparameters and structures that best suited for the deblurring task. We have used 12 layers of *ResNet* blocks. All filters have  $3 \times 3$  size, and the stride is 1. Therefore, the output of our model transformer is  $[64, 64, 256]$ .

**Decoder** The decoding works in the opposite way to the encoder. We reconstruct the image from the feature vectors by applying three deconvolution layers which use the reversed parameters of the encoding step. Therefore, the output of our model decoder is  $[256, 256, 3]$ .

### 3.2. Discriminative Network

The main goal of the discriminator is to extract features. It contains 5 convolutional layers. The hyperparameters of all the layers are the following: the total filters are  $[64, 128, 256, 5, 1]$ ; the stride is  $[2, 2, 2, 2, 1]$ ; and the activation function is *LeakyReLU* (slope = 0.2) for all the layers except for the last layer with *LeastSquareGAN*. All the filters have  $4 \times 4$  size. The principal role of discriminator is to decide whether these features belong to one particular category or not by the last layer, which is a convolutional layer with output  $1 \times 1$ .

### 3.3. Loss Function

There are two components of the CycleGAN objective function: an adversarial loss and a cycle consistency loss. Both are essential to obtaining good results. We train the models using *Least Square GAN* loss. To achieve our goal, the loss function must satisfy that the discriminator  $X$  should be trained for images as close as possible to domain  $X$ , and fake images close to 0. Thus, discriminator  $X$  would minimize  $(DiscriminatorX(x) - 1)^2$ . In the same way, it should be able to distinguish original and generated images. The discriminator must return 0 for images generated by the generator  $X$ . Discriminator  $X$  would minimize  $(DiscriminatorX(GeneratorY \rightarrow X(y)))^2$ .

On the other hand, generator  $X$  should be able to deceive discriminator  $Y$  about the authenticity of its generated images. This can be done if the recommendation by discriminator  $Y$  for the generated images is as close to 1 as possible. Therefore, generator  $X$  would like to minimize  $(DiscriminatorY(GeneratorX \rightarrow Y(x)) - 1)^2$ . And the most important cycle loss captures that we are able to get the image back using another generator and thus the difference between the original image and the cyclic image, which is  $[G_Y(G_X(x)) - x] + [G_X(G_Y(y)) - y]$ , should be as small as possible.

## 4. EXPERIMENTS

The following subsections describe the experiments that have been performed using the proposed “Blur2Sharp CycleGAN” method: the corpus of documents for training and testing together with the implementation details (see Section 4.1), and the results that have been obtained (see Section 4.2).

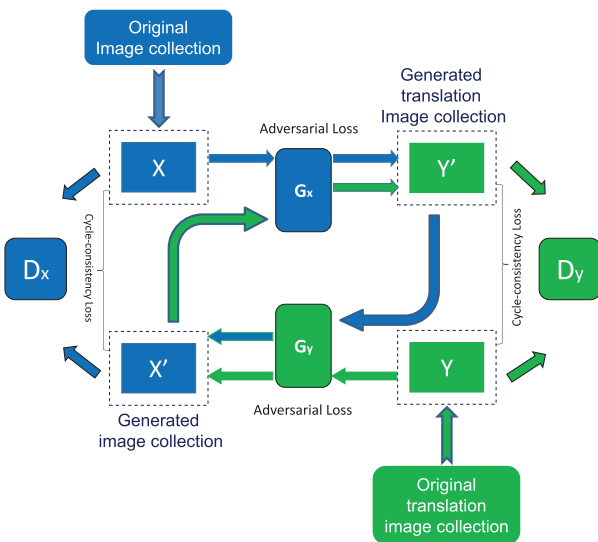


**Figure 2** | Cycle-consistent generative adversarial network (CycleGAN) approach.

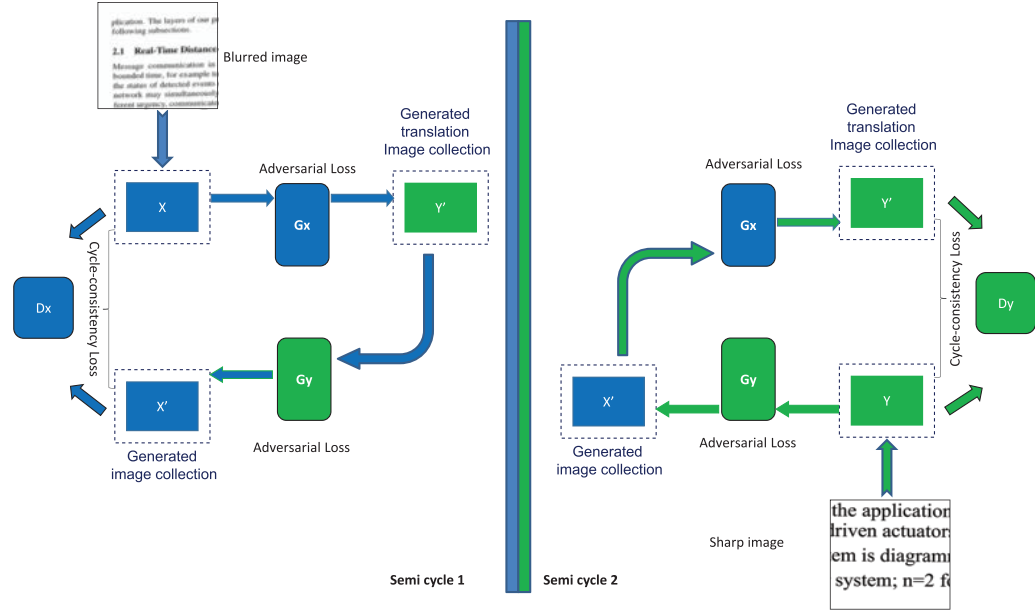


Figure 3 Training process for document image deblurring.

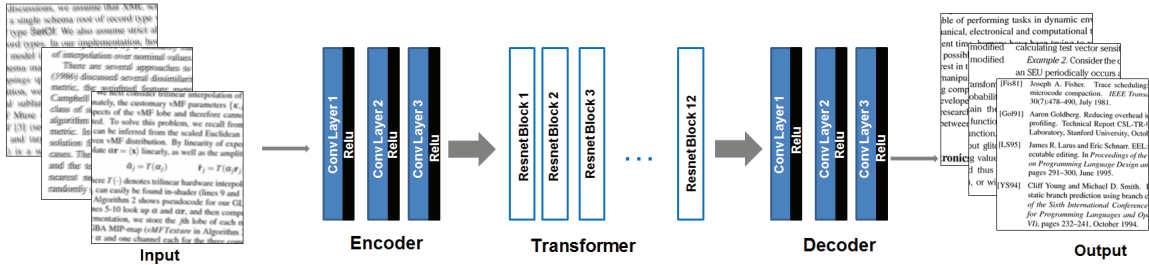


Figure 4 Our architecture for the two generator networks.

## 4.1. Datasets and Implementation

With respect to the unpaired dataset used for the experiments, we are using the dataset proposed by Hradiš *et al.* [13]. It consists of images with both defocus blur (using an uniform anti-aliased disc) and motion blur (generated by a random walk). We randomly cropped 2000 blurred image patches with  $256 \times 256$  size and 2001 cleaned image patches with  $256 \times 256$  size from the dataset for training.

For the testing phase, depicted in Figure 5, we used the test dataset proposed by Hradiš *et al.* [13], which includes 100 pairs of images (blurred images and their corresponding sharp versions) to evaluate the quality of image restoration.

We have implemented our Blur2Sharp Cycle-GAN on document deblurring in Python with the help of Keras and running the code on top of Google Tensorflow framework. In addition, it must be noted that all the computation works were run on an Ubuntu server with NVIDIA Quadro P6000 GPUs.

## 4.2. Results

Figure 6 shows two examples of the application of our “Blur2Sharp CycleGAN” method on the test dataset. Although the visual result

of sharp images seems satisfactory, it is difficult to distinguish visually a real image from a synthetic one when the differences between them are small. Therefore, we have compared quantitatively our method using two metrics: structural similarity index (SSIM) and peak signal to noise ratio (PSNR).

The computation of SSIM is shown in Eq. (1) including the following symbols:  $I$  is the structural similarity index;  $(x, y)$  are coordinates indicating a nearby  $N \times N$  window;  $\sigma_x, \sigma_y$  are the variances of intensities in  $x, y$  directions;  $\sigma_{xy}$  is the covariance; and  $\mu_x, \mu_y$  are the average intensities in  $x, y$  directions.

$$I(x, y) = \frac{(2\mu_x\mu_y + c_1)(2\sigma_{xy} + c_2)}{(\mu_x^2 + \mu_y^2 + c_1)(\sigma_x^2 + \sigma_y^2 + c_2)} \quad (1)$$

Eq. (2) shows the formula for computing PSNR, where  $MSE$  stands for the Mean Square Error,  $I_{ori}$  is the original image, and  $I_{deblur}$  is the deblurred image. MSE is computed according to Eq. (3), where  $m, n$  is the size of the image.

$$PSNR(I_{ori}, I_{deblur}) = 10 \log_{10} \frac{255^2}{MSE} \quad (2)$$



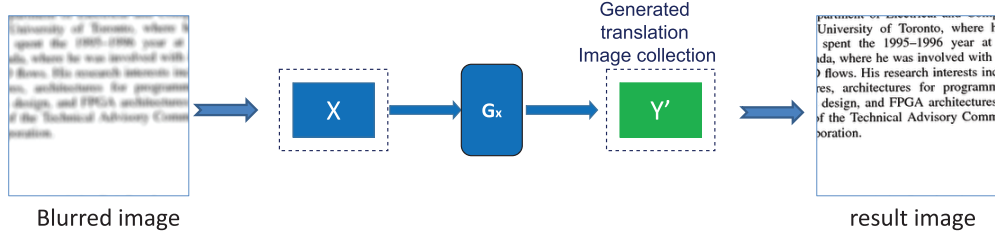


Figure 5 | Testing process.

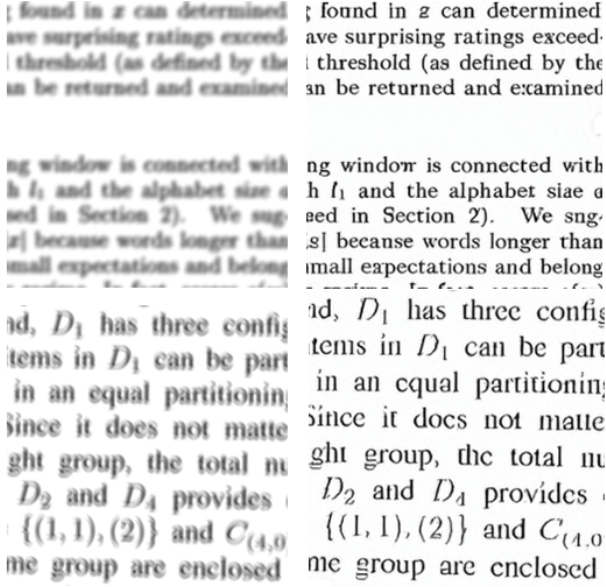


Figure 6 | Blur2Sharp cycle-consistent generative adversarial network (CycleGAN). From left to right: image blurred photo, result of Blur2Sharp CycleGAN.

$$MSE = \frac{1}{mn} \sum_{i=0}^{m-1} \sum_{j=0}^{n-1} [I_{ori}(i, j) - I_{deblur}(i, j)]^2 \quad (3)$$

Based on the two metrics defined above, we have compared the results obtained with our proposed Blur2Sharp CycleGAN architecture and the state-of-the-art methods using the test dataset previously described in Section 4.1: the 100 images extracted from the dataset proposed by Hradiš *et al.* [13]. The results are shown in Table 1. Our PSNR is equal to 32.52db and according to SSIM, we achieve 0.7689 on average using CycleGAN. Therefore, we can conclude that our “Blur2Sharp CycleGAN” has achieved a comparable SSIM and PSNR with the advantage of not having to use pairwise images for the training phase.

In addition, the results are good in terms of visual comparison with respect to the state-of-the-art. For instance, Figure 7 compares the results obtained with different methods on an input image that belongs to the text image deblurring dataset proposed by Hradiš *et al.* [13]. It can be observed that our Blur2Sharp CycleGAN method generates a sharp image with much clearer characters.

Table 1 | Quantitative comparison with state-of-the-art methods on the proposed image deblurring dataset.

	PSNR	SSIM
Pan <i>et al.</i> [5]	32.24	0.6627
Hradiš <i>et al.</i> [13]	33.40	0.9076
Pan <i>et al.</i> [14]	32.59	0.6708
Xu <i>et al.</i> [18]	20.12	0.8970
Blur2Sharp	32.52	0.7689
CycleGAN		

Finally, we have also compared the quality of the text obtained after applying an OCR algorithm on the output images generated by the different deblurring methods. After applying Tesseract software [21] to obtain OCR from the sharp images in the test dataset (used as reference text) and the images returned by the methods, we have computed the average cosine similarity between the character frequency vectors derived from each pair of corresponding OCR output files. We have considered only the detection of letters and digits within the range of printable characters in ASCII encoding. In this comparison we have also included the OCR obtained directly from blurred images to verify that deblurring is beneficial for OCR. As shown in Table 2, our method performs better than the methods of Pan *et al.* [5,14] and a bit worse than the method of Hradiš *et al.* [13]. It is logical that the method of Hradiš *et al.* performs better because it is a nonblind deconvolution method. It must also be noticed that the obtained OCR is not perfect, even for the sharp images in the testing dataset, because we are using cropped images with incomplete words and lines.

## 5. CONCLUSIONS

We presented a novel model that uses cycle-consistent adversarial networks for document deblurring. Our proposed “Blur2Sharp CycleGAN” architecture adjusts CycleGAN to the task of text image deblurring. We can both deblur images and blur sharp images because CycleGAN has the property of cycle-consistency. It is worth noting that since we use unpaired images as training dataset, we do not need the ground-truth sharp images. Based on our prior knowledge, successful image deblurring can be achieved with an unpaired image dataset using CycleGAN.

In addition, it must be noted that our model for image document deblurring obtains comparable results with respect to the current state-of-the-art. Moreover, the obtained PSNR values are at the same level as the best methods found in the research literature. This demonstrates that the idea of treating blur and sharpness as a kind

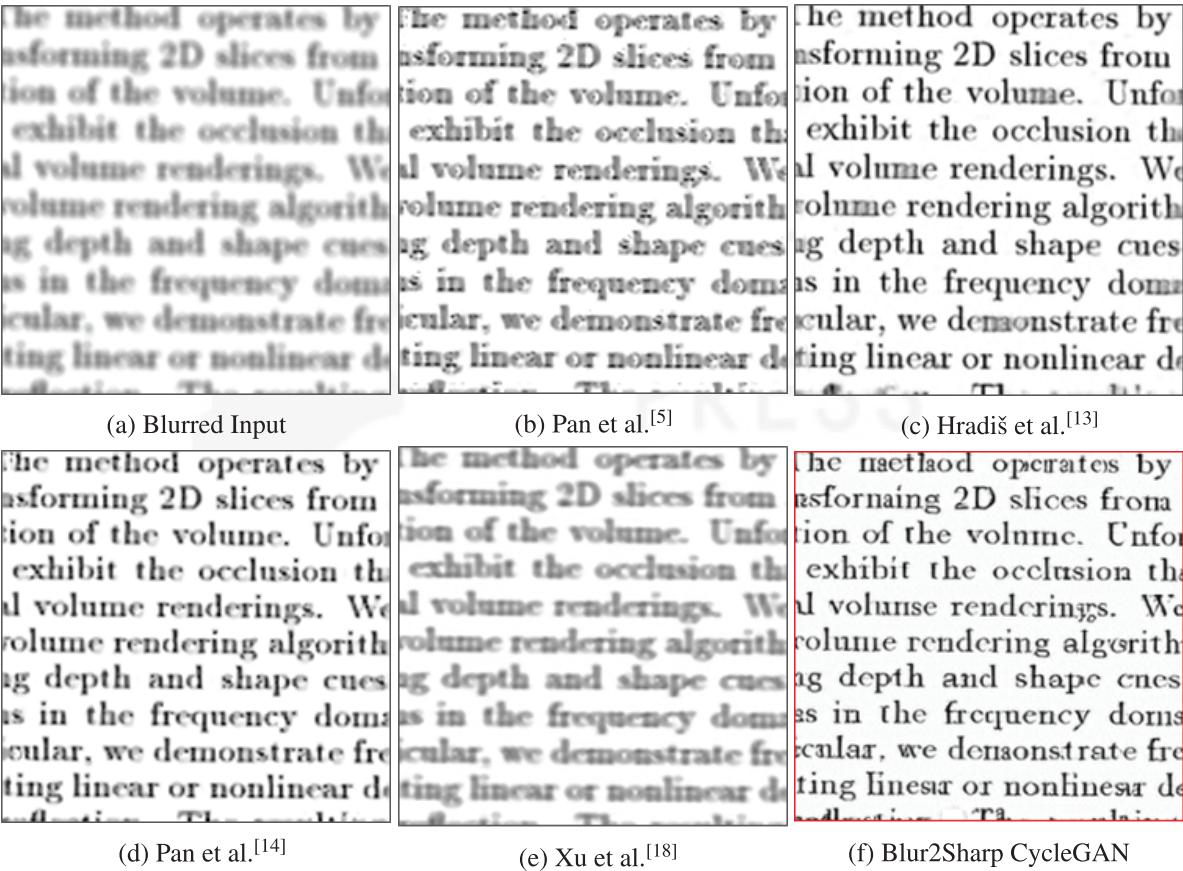


Figure 7 | Example of the outputs obtained after applying different deblurring methods.

Table 2	Quantitative comparison of OCR output.
Average Cosine Similarity	
No method (blurred images)	0.570
Pan et al. [5]	0.679
Pan et al. [14]	0.645
Hradiš et al. [13]	0.897
Blur2Sharp CycleGAN	0.872

of image style actually works. In addition, a by-product of generating fake blurring images using CycleGAN is also provided. Last, it must be noted that our model significantly improved the speed of the deblurring process thanks to GPU acceleration.

As future work we want to test the feasibility of “Blur2Sharp CycleGAN” as part of a more general task of historical document enhancement. Historical documents (and their digitized versions) suffer from several types of degradation that affect their readability and the application of OCR or text analysis processes. Apart from the noise originated by the bad conditions of original documents (e.g., stains or bad condition of paper), during the scanning (digitization) of pages from a bound book, the curving of the part of the page close to the “spine” introduces not only gutter shadows, but also out-of-focus blur in the shade area. Our aim is to verify whether “Blur2Sharp CycleGAN” can help to remove this kind of blur in this domain context.

CONFLICTS OF INTEREST

The authors declare of no conflicts of interest.

AUTHORS’ CONTRIBUTIONS

All authors have contributed to the design of the proposal for document image deblurring. Hala Neji has had the leading role in the implementation and execution of experiments. All authors have contributed to the edition of the manuscript.

ACKNOWLEDGMENTS

The research leading to these results has been partially supported by the Ministry of Higher Education and Scientific Research of Tunisia under the grant agreement number LR11ES48 and the Regional Government of Aragon (Spain, project T59 20R). In addition, we gratefully acknowledge the support of NVIDIA Corporation with the donation of the Quadro P6000 GPU used for this research.

REFERENCES

[1] P. Isola, J.-Y. Zhu, T. Zhou, A.A. Efros, Image-to-image translation with conditional adversarial networks, in Proceedings of the IEEE Conference on Computer Vision and Pattern Recognition (CVPR), Honolulu, HI, USA, 2017, pp. 1125–1134.

- [2] J.-Y. Zhu, T. Park, P. Isola, A.A. Efros, Unpaired image-to-image translation using cycle-consistent adversarial networks, in *Proceedings of the IEEE International Conference on Computer Vision*, Venice, Italy, 2017, pp. 2223–2232.
- [3] X. Chen, X. He, J. Yang, Q. Wu, An effective document image deblurring algorithm, in *Conference on Computer Vision and Pattern Recognition (CVPR 2011)*, IEEE, Colorado Springs, CO, USA, 2011, pp. 369–376.
- [4] H. Cho, J. Wang, S. Lee, Text image deblurring using text-specific properties, in *European Conference on Computer Vision*, Springer, Florence, Italy, 2012, pp. 524–537.
- [5] J. Pan, Z. Hu, Z. Su, M.-H. Yang, Deblurring text images via L0-regularized intensity and gradient prior, in *Proceedings of the IEEE Conference on Computer Vision and Pattern Recognition*, Columbus, OH, USA, 2014, pp. 2901–2908.
- [6] N. Nayef, P. Gomez-Kramer, J.-M. Ogier, Deblur-ring of document images based on sparse representations enhanced by non-local means, in *2014 22nd International Conference on Pattern Recognition*, IEEE, Stockholm, Sweden, 2014, pp. 4441–4446.
- [7] M. Zhang, C. Desrosiers, C. Zhang, M. Cheriet, Effective document image deblurring via gradient histogram preservation, in *2015 IEEE International Conference on Image Processing (ICIP)*, IEEE, Quebec City, Canada, 2015, pp. 779–783.
- [8] M. Ljubenovic, L. Zhuang, M.A. Figueiredo, Class-adapted blind deblurring of document images, in *2017 14th IAPR International Conference on Document Analysis and Recognition (ICDAR)*, IEEE, Kyoto, Japan, 2017, vol. 1, pp. 721–726.
- [9] J. Pan, J. Dong, Y.-W. Tai, Z. Su, M.-H. Yang, Learning discriminative data fitting functions for blind image deblurring, in *Proceedings of the IEEE International Conference on Computer Vision*, Venice, Italy, 2017, pp. 1068–1076.
- [10] X. Jiang, H. Yao, S. Zhao, Text image deblurring via two-tone prior, *Neurocomputing*, 242 (2017), 1–14.
- [11] Y. Liu, S. Liu, C. Li, D. Yang, Compressed sensing image reconstruction based on convolutional neural network, *Int. J. Comput. Intell. Syst.* 12 (2019), 873–880.
- [12] W. Wei, J. Yongbin, L. Yanhong, L. Ji, W. Xin, Z. Tong, An advanced Deep Residual Dense Network (DRDN) approach for image super-resolution, *Int. J. Comput. Intell. Syst.* 12 (2019), 1592–1601.
- [13] M. Hradiš, J. Kotera, P. Zemčík, F. Šroubek, Convolutional neural networks for direct text deblurring, in *Proceedings of British Machine Vision Conference (BMVC)*, Swansea, UK, 2015, vol. 10, p. 2.
- [14] J. Pan, D. Sun, H. Pfister, M.-H. Yang, Blind image deblurring using dark channel prior, in *Proceedings of the IEEE Conference on Computer Vision and Pattern Recognition*, Las Vegas, NV, USA, 2016, pp. 1628–1636.
- [15] B. Fu, L. Wang, R. Wang, S. Fu, F. Liu, X. Liu, Underwater image restoration and enhancement via residual two-fold attention networks, *Int. J. Comput. Intell. Syst.* 14 (2021), 84–95.
- [16] T.B. Lee, S.H. Jung, Y.S. Heo, Progressive semantic face deblurring, *IEEE Access*, 8 (2020), 223548–223561.
- [17] Q. Guo, W. Feng, R. Gao, Y. Liu, S. Wang, Exploring the effects of blur and deblurring to visual object tracking, *IEEE Trans. Image Process.* 30 (2021), 1812–1824.
- [18] X. Xu, D. Sun, J. Pan, Y. Zhang, H. Pfister, M.-H. Yang, Learning to super-resolve blurry face and text images, in *Proceedings of the IEEE International Conference on Computer Vision*, Venice, Italy, 2017, pp. 251–260.
- [19] M.T. Nimisha, K. Sunil, A. Rajagopalan, Unsupervised class-specific deblurring, in *Proceedings of the European Conference on Computer Vision (ECCV)*, Munich, Germany, 2018, pp. 353–369.
- [20] B. Lu, J.-C. Chen, R. Chellappa, Unsupervised domain-specific deblurring via disentangled representations, in *Proceedings of the IEEE Conference on Computer Vision and Pattern Recognition*, Long Beach, CA, USA, 2019, pp. 10225–10234.
- [21] Google Open Source, Tesseract OCR, 2021. <https://opensource.google/projects/tesseract>